

# Correlations at intermediate $p_T$

**Rudolph C. Hwa**

Institute of Theoretical Science and Department of Physics  
University of Oregon, Eugene, OR 97403-5203, USA

E-mail: hwa@uoregon.edu

**Abstract.** Correlations among hadrons in jets produced in heavy-ion collisions are discussed in the framework of the recombination model. The basic correlation at the parton level is among the shower partons arising from kinematical constraint. The resultant correlation between hadrons at intermediate  $p_T$  is amazingly rich in characteristics.

## 1. Introduction

The study of the correlations at intermediate  $p_T$  in heavy-ion collisions at high energy is important for the understanding of the interaction between a hard parton and the hot dense medium that it traverses. By intermediate  $p_T$  we mean the region that stands between the soft region ( $p_T < 2$  GeV/c) where the recombination of thermal partons is most important and the hard region ( $p_T > 9$  GeV/c) where the fragmentation of partons is dominant. Note that this classification of regions is determined by the modes of hadronization, which we shall review briefly, rather than by the nature of scattering, soft or hard. In the intermediate  $p_T$  region the recombination of the thermal and shower partons is more important than any other component of hadronization and clearly conveys the medium effect on hard partons. And it is in that region where the recent analysis of the data from RHIC reveals a wealth of information on jet structure. We shall examine the properties of correlation in the framework of parton recombination, which is the only viable hadronization scheme that can account for the species dependence of the particles produced. Our emphasis will be on near-side correlation, which depends mainly on the correlation among shower partons in a jet. The away-side correlation involves other issues besides hadronization and will be the subject of a future investigation.

## 2. Single-particle distribution

Before discussing two-particle correlation, it is fitting to review first the single-particle distribution as determined in the recombination model [1]. In that model the shower partons in a jet play a crucial role. They are semi-hard and can recombine with soft thermal partons on the one hand, and also with one another on the other hand. Their distributions cannot be calculated in perturbative QCD, but can be determined phenomenologically from the fragmentation functions (FF), which are themselves determined by fitting the fragmentation processes in the collisions of simple systems. In the framework of parton recombination the shower parton distributions (SPD) can be extracted from the fragmentation function  $D(x)$  by

use of the equation [2]

$$xD_i^\pi(x) = \int \frac{dx_1}{x_1} \frac{dx_2}{x_2} \left\{ S_i^j(x_1), S_i^{j'}\left(\frac{x_2}{1-x_1}\right) \right\} R_\pi(x_1, x_2, x) \quad , \quad (1)$$

where  $i$  specifies the type of hard parton that fragments,  $j$  and  $j'$  denotes the types of two partons that recombine, and  $R_\pi$  is the recombination function (RF) for the formation of a pion. The two SPDs,  $S_i^j$  and  $S_i^{j'}$ , are symmetrized in the order of emission with momentum fractions  $x_1$  and  $x_2$  [see (12) below for the details]. Five such parton distributions have been determined from five types of  $D(x)$  functions [2]. The RF for pion is [3]

$$R_\pi(x_1, x_2, x) = \frac{x_1 x_2}{x} \delta(x_1 + x_2 - x), \quad (2)$$

and is inferred from pion-induced Drell-Yan process; for proton formation the details are given also in [3].

In heavy-ion collisions the probability of finding a shower parton  $j$  is [1]

$$\mathcal{S}^j(q) = \xi \sum_i \int dk k f_i(k) S_i^j(q/k) \quad , \quad (3)$$

where  $f_i(k)$  is the probability of producing a hard parton of species  $i$  at transverse momentum  $k$  [4].  $\xi$  is the average fraction of the number of hard partons that emerge from the bulk medium to hadronize in vacuum.

The thermal parton distribution (TPD) is determined by fitting the soft pion distribution at  $p_T < 2$  GeV/c by use of the recombination formula

$$\frac{dN_\pi}{p dp} = \frac{1}{p^2} \int \frac{dq_1}{q_1} \frac{dq_2}{q_2} F_{q\bar{q}}(q_1, q_2) R_\pi(q_1, q_2, p) \quad (4)$$

where  $p_T$  is denoted by  $p$ , for brevity. For TPD we use the factorizable form

$$F_{q\bar{q}}(q_1, q_2) = \mathcal{T}(q_1) \mathcal{T}(q_2) \quad , \quad (5)$$

where

$$\mathcal{T}(q) = C q e^{-q/T}. \quad (6)$$

It is found from the low- $p_T$  data of pions that [1]

$$C = 23.2 (\text{GeV}/c)^{-1}, \quad T = 0.317 \text{ GeV}/c \quad (7)$$

for central Au-Au collisions. For non-central collisions the parameters are given in [5].

With these basic quantities specified we can now describe how the pion distribution can be determined for any  $p_T$  by use of the same equation (4), but with the two-parton distribution generalized to include the shower partons.

$$F_{q\bar{q}}(q_1, q_2) = \mathcal{T}(q_1) \mathcal{T}(q_2) + \mathcal{T}(q_1) \mathcal{S}(q_2) + \mathcal{S}\mathcal{S}(q_1, q_2) \quad (8)$$

where the last term is written in that way to emphasize that it is not factorizable, i.e.,

$$(\mathcal{S}\mathcal{S})(q_1, q_2) = \xi \sum_i \int dk k f_i(k) \left\{ S_i\left(\frac{q_1}{k}\right), S_i\left(\frac{q_2}{k-q_1}\right) \right\} \quad . \quad (9)$$

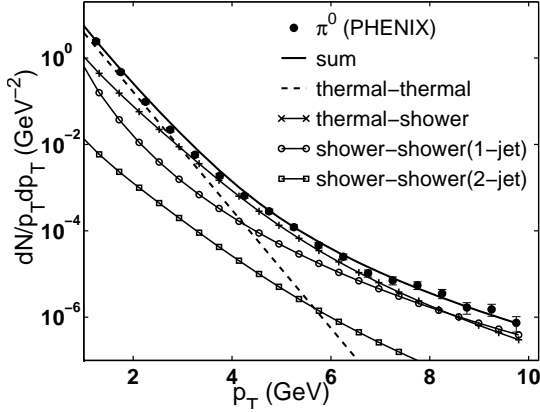


**Figure 1.** Transverse momentum distribution of  $\pi^0$  in Au-Au collisions. Data in solid circles are from [6].

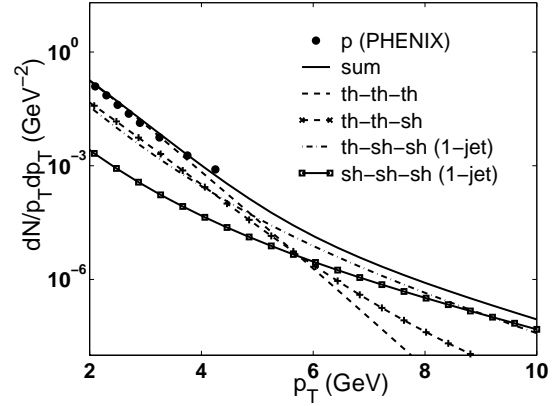


**Figure 2.** Transverse momentum distribution of proton in Au-Au collisions. Data in solid circles are from [6].

In view of (1) and (4) it should be clear that the  $\mathcal{SS}$  terms in  $F_{q\bar{q}}$  leads to fragmentation

$$\frac{dN_{\pi}^{\mathcal{SS}}}{pd p} = \frac{\xi}{p} \sum_i \int dk f_i(k) D_i^{\pi} \left( \frac{p}{k} \right) . \quad (10)$$

What is new is the  $\mathcal{TS}$  term in (8); it dominates in the intermediate  $p_T$  region, as evidenced in Fig. 1, in which the overall normalization is adjusted to fit the data [6] by letting  $\xi$  be 0.07. The shape of the  $p_T$  dependence is a prediction of the model. In that figure the shower-shower (2 jet) line corresponds to the recombination of shower partons arising from two different jets, and should be ignored for collisions at RHIC energies. The dominance of  $\mathcal{TS}$  recombination in the  $3 < p_T < 9$  GeV/c region cannot be reproduced by fragmentation even if the FF used is medium-modified because the momentum fraction  $x$  in the FF requires the parton momentum to be greater than the pion momentum  $p$ , whereas the RF requires the coalescing parton momenta to be less than  $p$ . Since the parton momenta are damped by a power law, the latter process always wins.

The contrast between the two processes of hadronization becomes even more pronounced in the case of proton production. Since three quarks recombine to form a proton, the average parton momentum is  $p/3$ , so they are even more abundantly available. To form a proton by fragmentation, one pays a heavy penalty to produce a high  $k$  parton, and then pays an even heavier penalty to require that it fragments into a proton, the FF for which is an order of magnitude smaller than  $D^{\pi}$ . This is why the  $p/\pi$  ratio can be high in the recombination model but very small in the fragmentation model. The production of proton in central AuAu collisions has been calculated in the recombination model where  $\mathcal{TTS}$  and  $\mathcal{TSS}$  components have been found to be more important than  $\mathcal{SSS}$  component (i.e., fragmentation) for  $p_T < 9$  GeV/c [1]. This is shown in Fig. 2, where the data [6] exist only up to 4 GeV/c. But that is enough to exhibit the large  $p/\pi$  ratio [7], as shown in Fig. 3, where the dashed line takes the proton mass into account at low  $p_T$  [1]. Actually, the large  $p/\pi$  ratio was obtained in an earlier paper on recombination [8] even before the shower parton distributions were obtained. The parton distributions there were inferred from the pion distribution. Two other groups have also obtained similar results using recombination/coalescence model [9, 10].

The Cronin effect has for thirty years been referred to as the manifestation of  $k_T$  broadening by multiple scattering in the initial state of pA collisions. That relationship does not take into account of the fact that the experimental  $p_T$  spectrum in  $p + A \rightarrow h + X$  depends on  $A$  as

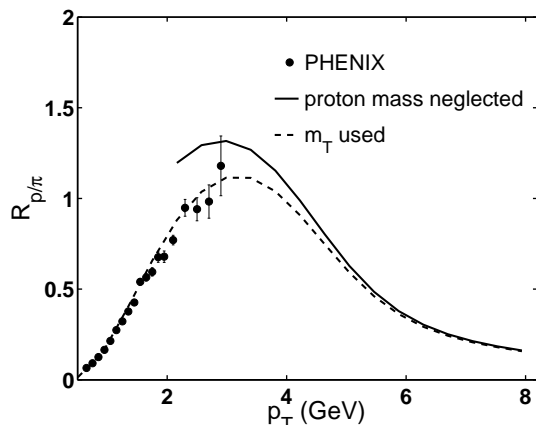


**Figure 3.** Comparison of calculated  $p/\pi$  ratio with data from [7] on AuAu collisions.

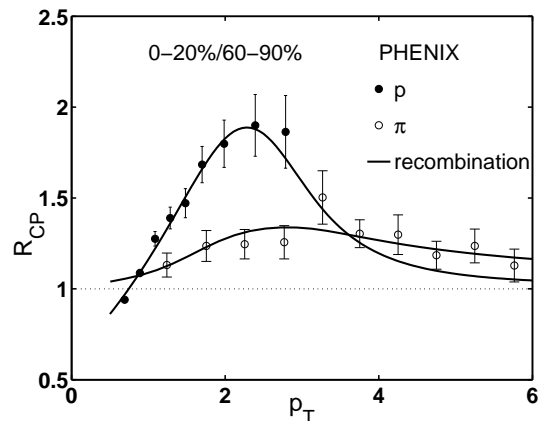


**Figure 4.**  $R_{CP}$  for proton and pion in d-Au collisions. The data are from [13].

$A^{\alpha_h}$ , where  $\alpha_p > \alpha_\pi$  [11]. If the effect of the nuclear medium on hard scattering is before fragmentation, then the exponent  $\alpha_h$  should be independent of whether the hadron  $h$  is a pion or a proton. In reality, not only is  $\alpha_p > \alpha_\pi$  experimentally, the FF for proton  $D^p$  is much smaller than that for pion,  $D^\pi$ , by roughly an order of magnitude. This failure in interpreting the data has been corrected by use of parton recombination as the hadronization mechanism. We have studied the production of hadrons (pion and proton) at intermediate  $p_T$  in d-Au collisions at all centralities in the recombination model [12]. Fig. 4 shows our results on  $R_{CP}$  for pion and proton. Evidently, we obtain  $R_{CP}^p > R_{CP}^\pi$  in the range  $1 < p_T < 3$  GeV/c, in good agreement with the data [13]. This result may be regarded as the strongest support for the recombination model, since no other approaches have indicated the possibility of attaining the same.

One last feature of single-particle distributions that we choose to mention here is the suppression of  $R_{CP}$  in forward production. BRAHMS data on d-Au collision [14] have shown that  $R_{CP}$  is as low as 0.5 at  $\eta = 3.2$ . Such a suppression of central production has been interpreted as suggestive evidence for color glass condensate, since at large  $\eta$  the small- $x$  nuclear partons are presumed to be important and their high density there reveals saturation physics. We have, however, calculated the  $p_T$  spectra at large  $\eta$  in the recombination model without incorporating any exotic physics, and found results in agreement with the data [14, 15]. Our input is the data on  $dN_{ch}/d\eta$  which decreases with increasing  $\eta$  much more rapidly for central d-Au collisions than for peripheral collisions. Since  $dN_{ch}/d\eta$  is dominated by soft partons, the  $\mathcal{TS}$  recombination results in the corresponding decrease of the hadron distributions at large  $\eta$ . There is no change of the underlying physics as  $\eta$  is carried from backward to forward direction.

### 3. Parton and hadron correlations in jets

Having established some degree of reliability of parton recombination in the treatment of single-particle distributions, we now consider correlation of particles in jets at high  $p_T$ . There are two ways to study correlation: one is to use trigger particles to select events in which the associated particles reveal near-side and away-side characteristics; the other is to treat the two particles on equal footing and study the two-particle correlation function. Both approaches have been adopted by different groups within the STAR collaboration. We have some recent results on both that can be reported here, starting with the latter.

In general, the two-particle correlation is defined by

$$C_2(1, 2) = \rho_2(1, 2) - \rho_1(1)\rho_1(2) \quad . \quad (11)$$

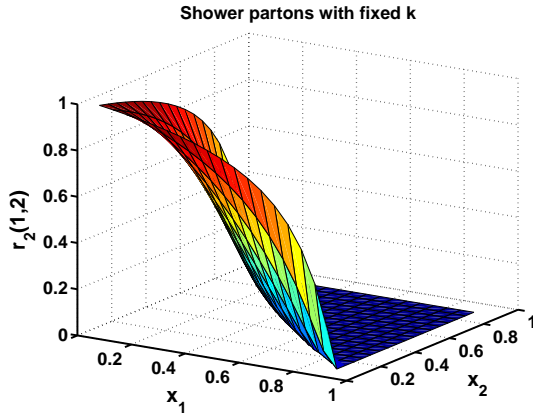


**Figure 5.** The ratio  $r_2(1,2)$  in terms of the momentum fractions of two shower partons in a hard gluon jet.

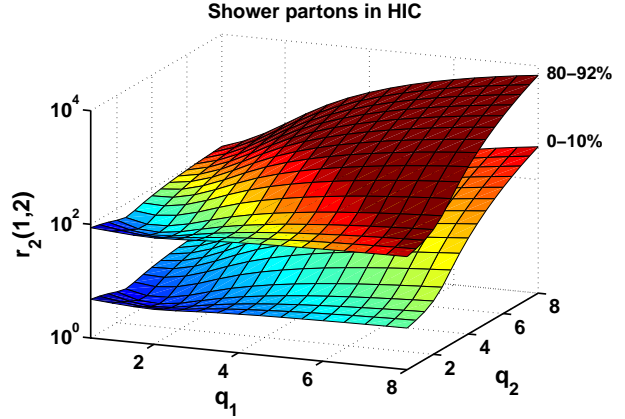


**Figure 6.** The ratio  $r_2(1,2)$  in terms of the momenta of two shower partons in heavy-ion collisions for two extreme centralities.

where  $\rho_2(1,2)$  is the two-particle distribution, and  $\rho_1(1)$  is the one-particle distribution, which for pion production at intermediate  $p_T$  is given by (4) in the recombination model. It is, however, more appropriate to discuss first, not particle correlation, but parton correlation in a jet. Consider a hard parton with a fixed momentum  $k$  in vacuum, as in  $e^+e^-$  annihilation. Since we shall discuss the correlation in terms of momentum fractions  $x_i$ , it does not matter what  $k$  is so long as it is high enough. Thus for a single shower parton, we have  $\rho_1(1) = S_i^j(x_1)$ .

For two shower partons we have

$$\rho_1(1,2) = \left\{ S_i^j(x_1), S_i^{j'}\left(\frac{x_2}{1-x_1}\right) \right\} = \frac{1}{2} \left[ S_i^j(x_1) S_i^{j'}\left(\frac{x_2}{1-x_1}\right) + S_i^j\left(\frac{x_1}{1-x_2}\right) S_i^{j'}(x_2) \right] \quad (12)$$

which guarantees that  $x_1 + x_2 \leq 1$  and symmetrizes the order of emission. Evidently, the two partons are correlated by virtue of the form in (12). If we define the normalized distribution by the ratio

$$r_2(1,2) = \frac{\rho_2(1,2)}{\rho_1(1)\rho_1(2)} \quad , \quad (13)$$

then the result of our calculation for  $r_2(1,2)$  is shown in Fig. 5 [5]. It is clear that there is correlation for almost all  $x_1$  and  $x_2$  except when they are very small, where  $r_2(1,2) \approx 1$ .

Now, consider two shower partons in a jet in heavy-ion collisions. In that case the hard parton momentum  $k$  is not fixed, so the corresponding  $\rho_1$  and  $\rho_2$  involve integrals over  $k$ , i.e.,

$$\rho_1(1) = \mathcal{S}(q_1) \quad , \quad \rho_2(1,2) = (\mathcal{S}\mathcal{S})^{jj'}(q_1, q_2) \quad , \quad (14)$$

where  $\mathcal{S}$  and  $\mathcal{S}\mathcal{S}$  are given in (3) and (9). The calculated results for  $r_2(1,2)$  in that case are shown in Fig. 6 for both central and peripheral collisions [5]. They become very large at large  $q_1$  and  $q_2$  because each  $\rho_1$  is power damped at large  $k$ , as is  $\rho_2$ . The drastic difference between Figs. 5 and 6 underscores the effect of hard scattering in heavy-ion collision even when the only correlation in the problem is the same in both cases.

The correlation between pions in jets is far more complicated to calculate because of the many ways that partons can recombine. The two-pion distribution is

$$\rho_2(1,2) = \frac{dN_{\pi_1\pi_2}}{p_1 p_2 dp_1 dp_2} = \frac{1}{(p_1 p_2)^2} \int \left( \prod_i \frac{dq_i}{q_i} \right) F_4(q_1, q_2, q_3, q_4) R(q_1, q_3, p_1) R(q_2, q_4, p_2). \quad (15)$$

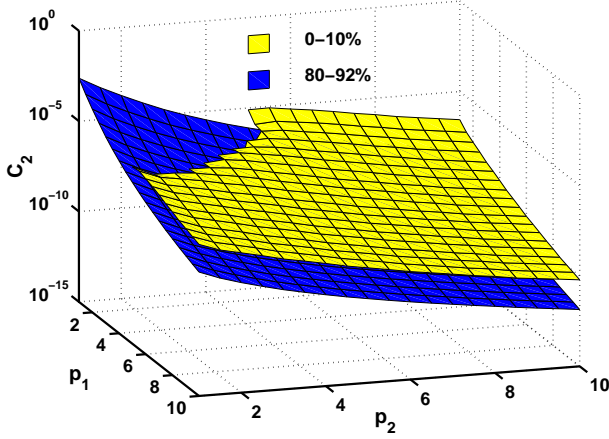


**Figure 7.** The correlation function  $C_2$  for two centralities when they are positive. At low values of  $p_1$  and  $p_2$ ,  $C_2$  becomes negative for central collisions.

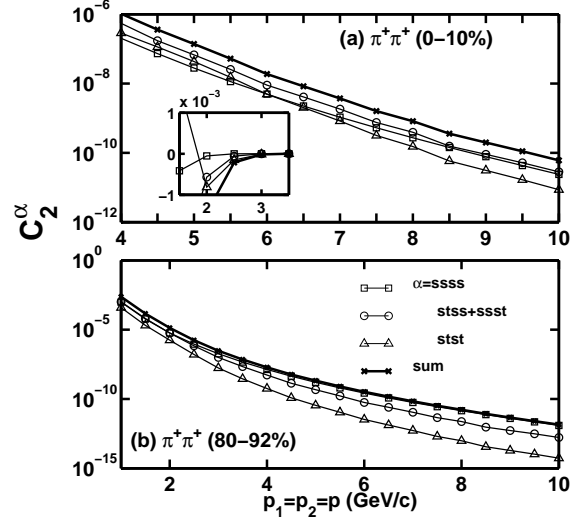


**Figure 8.** The correlation function  $C_2$  for (a) central and (b) peripheral collisions along the diagonal where  $p_1 = p_2$ .

where

$$F_4 = (\mathcal{T}\mathcal{T} + \mathcal{S}\mathcal{T} + \mathcal{S}\mathcal{S})_{13}(\mathcal{T}\mathcal{T} + \mathcal{S}\mathcal{T} + \mathcal{S}\mathcal{S})_{24} \quad . \quad (16)$$

While many parts of  $F_4$  are factorizable, and therefore make no contribution to  $C_2(1, 2)$ , there are non-factorizable parts that involve at least one  $\mathcal{S}$  in each of  $(\cdots)_{13}$  and  $(\cdots)_{24}$ , the most important example of which is  $(\mathcal{S}\mathcal{T})_{13}(\mathcal{S}\mathcal{T})_{24}$ . The two  $\mathcal{S}$  terms in that component, involving the shower partons  $S(q_1)$  and  $S(q_2)$  are correlated because they are in the same jet. Using (15) and (4) in (11), we obtain  $C_2(1, 2)$  which is shown in Fig. 7. There is not too much difference in the shapes of  $C_2$  for the central and peripheral cases for most of  $p_1$  and  $p_2$ , except when the momenta are small where  $C_2$  becomes negative for central collisions and therefore cannot be exhibited in the log plot [5]. The rapid decrease at large momenta is due to the power-law damping of  $f_i(k)$  in both  $\rho_1$  and  $\rho_2$ . In the lower part of the intermediate  $p_T$  region various components of  $C_2$  become negative, as shown in Fig. 8. That occurs because of the competition for the shower parton momenta in a jet, when the hard parton momentum  $k$  can be low enough to avoid the severe suppression of  $f_i(k)$ . Since the correlation of the shower partons is negative, as we have seen in Fig. 5, it is not surprising that  $C_2$  for the hadrons also becomes negative when  $p_1$  and  $p_2$  are not too high.

To compensate for that suppression at high  $p_T$  let us define

$$G_2(1, 2) = \frac{C_2(1, 2)}{[\rho_1(1)\rho_1(2)]^{1/2}} \quad , \quad (17)$$

whose dependence on  $p_1$  and  $p_2$  can now be shown in linear plots. Fig. 9(a) shows that for central collisions  $G_2$  becomes negative for  $p_1$  and/or  $p_2 \lesssim 4$  GeV/c. The ratio,  $R_{CP}^{G_2}$ , of  $G_2$  for the two extreme centralities exhibits a minimum at  $p_1 \approx p_2 \approx 2$  GeV/c, as shown in Fig. 9(b) [5]. Data on that ratio, thus far not analyzed, would be able to provide information on whether there exist any dynamical correlations that we have not incorporated in our calculation.

So far we have only considered the correlations in the momentum variables  $p_1$  and  $p_2$  of  $C_2(1, 2)$ . We can also study the autocorrelation in  $\Delta\eta$  and  $\Delta\phi$ , for which there are data at low

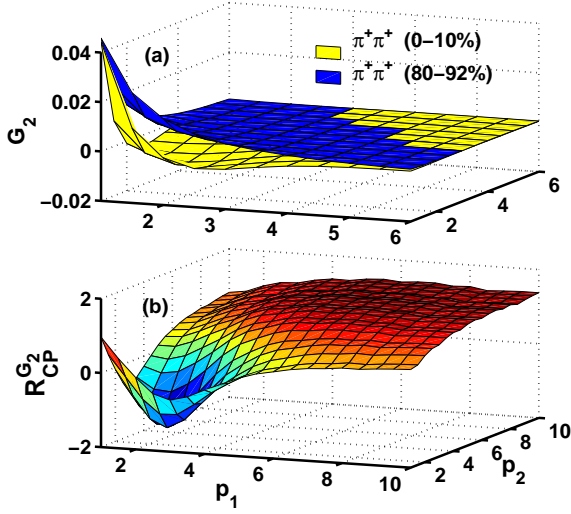


**Figure 9.** (a)  $G_2(1,2)$  for two centralities. (b) The ratio  $R_{CP}^{G_2}$  of central to peripheral  $G_2$ .

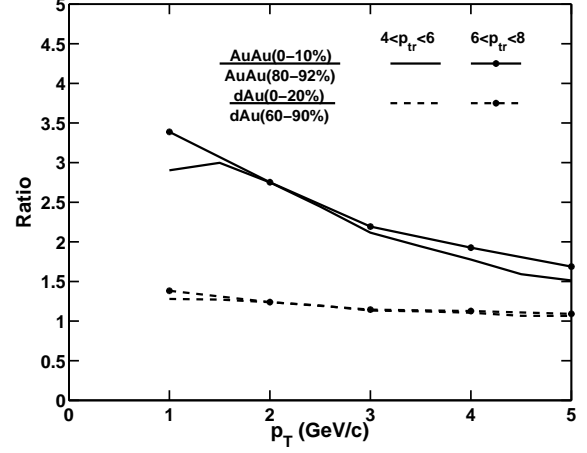


**Figure 10.**  $R_{CP}$  vs the momentum of the AP ( $\pi^+$ ) for two trigger windows.

$p_T$  [16]. For such studies we need information on the angular distribution of shower partons. With that goal in mind we turn next to the investigation of correlations with trigger particles selected to serve as reference.

#### 4. Associated particle distributions

If we use  $p_1$  to denote the transverse momentum of the trigger, and  $p_2$  that of the associated particle, then the per-trigger distribution of the latter for pions is

$$\frac{dN_{\pi}^{AP}}{p_2 dp_2} = \frac{\int dp_1 p_1 \frac{dN_{\pi\pi}}{p_1 p_2 dp_1 dp_2}}{\int dp_1 p_1 \frac{dN_{\pi}}{p_1 dp_1}}, \quad (18)$$

where  $p_1$  is integrated over a range that corresponds to the experimental cut on the trigger momentum. The integrands in the numerator and denominator are, respectively, (15) and (4). The associated particle distribution (APD) has been calculated for both dAu and AuAu collisions at various centralities [17]. It is found that the  $p_T$  distribution of the APD for dAu collisions has negligible dependence on centrality, although the dependence is quite significant for AuAu collisions. Those results are summarized in Fig. 10. They are different from the results reported in [18] because different quantities are calculated: whereas (18) corresponds to the ratio of integrals, that in [18] is the integral of the ratio. Comparison with the experimental data should be made only when the appropriate quantity is chosen that corresponds to what is measured and analyzed.

Let us now go on to the angular dependence of the APD. To exhibit the structures of the near- and away-side jets, it is necessary to make background subtraction of the data. F. Wang has presented data on  $\Delta\phi$  and  $\Delta\eta$  distributions, where the subtraction scheme used results in the vanishing of the APD in  $\Delta\phi$  at  $|\Delta\phi| = 1$  [19]. The corresponding distribution in  $\Delta\eta$  shows a pedestal on top of which sits a peak at  $\Delta\eta = 0$ . To address these features found in the data it is necessary for us to generalize the formalism that we have used for recombination. So far our consideration has only been one-dimensional (1D), where the parton and hadron momenta are all collinear. Now we must consider shower partons in a jet cone that has 3D characteristics. Furthermore, we must take into account the energy loss of the hard partons

and the subsequent hadronization of the medium that has absorbed the radiated energy. These aspects of generalization have been considered in [20].

The fact that the APD in  $\Delta\eta$  has a pedestal, not found in the  $\Delta\phi$  distribution, suggests the basic lack of symmetry between the longitudinal and azimuthal directions. Indeed, whereas there is longitudinal expansion of the compressed medium, there is no azimuthal expansion in the transverse plane, only radial expansion. That means that there is no mixing of the various  $\phi$  sectors, making possible the implication that the particles detected in the peak region with  $|\Delta\phi| < 1$  arise from partons, soft or hard, that are originally in the same  $\phi$  sector, i.e., where the trigger is measured in the azimuth. That is not the case with the  $\eta$  variable due to longitudinal expansion, and therein lies the possibility of a pedestal outside the peak region in  $\Delta\eta$  where the trigger is.

Endowing the parton momenta with vectorial properties in 3D, we use  $\psi$  to denote the angle between  $\vec{q}_2$  and  $\vec{k}$ , assuming for simplicity that  $\vec{q}_1$  is along  $\vec{k}$ , based on the recognition that it is the relative angle between  $\vec{q}_1$  and  $\vec{q}_2$  that matters. We further assume that there is enough dispersion of the thermal partons around the average direction at any  $(\eta, \phi)$  such that the hadron momenta  $\vec{p}_1$  and  $\vec{p}_2$  due to  $\mathcal{TS}$  recombination can be directed along  $\vec{q}_1$  and  $\vec{q}_2$ , respectively. That means that  $\psi$  is also the angle between the measured pion momenta. Consequently, it is possible to relate  $\psi$  to the pseudorapidities  $\eta_1$  and  $\eta_2$ . Let us describe the angular distribution of the shower partons around the jet axis by a Gaussian

$$G(\psi, x) = \exp \left[ -\psi^2 / 2\sigma^2(x) \right] \quad , \quad (19)$$

where the width depends on the momentum fraction  $x$  as

$$\sigma(x) = \sigma_0(1 - x) \quad , \quad (20)$$

which is a simple way to capture the property that the jet cone is wider for softer partons.  $\sigma_0$  is a free parameter that is to be determined phenomenologically.

With the angular variable described above we can now write down the contribution to  $F_4$  that gives rise to the trigger at  $\vec{p}_1$  and the AP at  $\vec{p}_2$  within the peak in  $\Delta\eta$  through  $\mathcal{TS}$  recombination for both pions

$$F_4^{TSTS} = \xi \sum_i \int dk k f_i(k) \mathcal{T}(q_3) \{S(q_1), S(q_2)\} \mathcal{T}(q_4) G(\psi, q_2/k) \quad (21)$$

where  $q_1$  and  $q_3$  form the trigger at  $p_1$ , and  $q_2$  and  $q_4$  form the AP at  $\vec{p}_2$  at an angle  $\psi$  relative to  $\vec{p}_1$ .  $\mathcal{T}(q)$  has the same form as in (6), but the inverse slope  $T$  is now allowed to be higher than the value used in the past in order to take into account the enhanced thermal distribution due to the loss of energy of the hard parton while traversing the medium. Since the enhanced thermal partons are in the immediate vicinity of the hard parton, they are the ones that recombine with the shower partons, as expressed in (21). How  $T$  differs from the value  $T_0$  determined from the soft hadron distribution for  $p_T < 2$  GeV/c without being in the presence of any jet is another parameter  $\Delta T$  in the problem. We determine  $\Delta T$  from the pedestal height. In the recombination model we are able to attribute the pedestal effect to the difference of  $\mathcal{TT}$  recombination when there is a jet and  $\mathcal{T}_0\mathcal{T}_0$  recombination of the background in the absence of a jet. That is, for the pedestal we have

$$F_4^{ped} = \xi \sum_i \int dk k f_i(k) S(q_1) \mathcal{T}(q_3) [\mathcal{T}(q_2) \mathcal{T}(q_4) - \mathcal{T}_0(q_2) \mathcal{T}_0(q_4)] \quad (22)$$

where the part before the square brackets is for the trigger as in (21), while the quantity inside the square brackets is what remains of the thermal partons for recombination after background



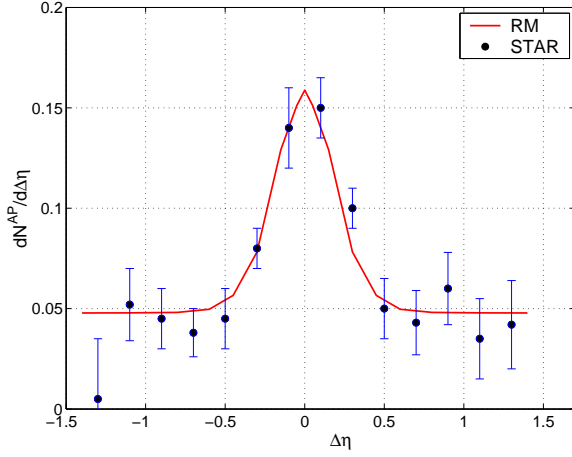


**Figure 11.** APD in  $\Delta\eta$  for  $2 < p_T < 4$  GeV/c with trigger particle in  $4 < p_T^{trig} < 6$  GeV/c. The data from [19] are for all charged hadrons in the respective  $p_T$  ranges.

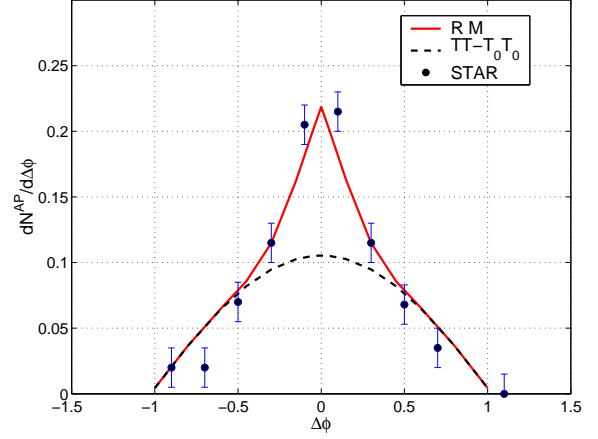


**Figure 12.** Same as in Fig. 11 except that the distribution is in  $\Delta\phi$ . The dashed line represents the pedestal effect in  $\Delta\phi$ .

subtraction. Using the value  $T_0 = 0.317$  GeV/c we can determine  $T = T_0 + \Delta T$  by varying  $\Delta T$  to fit the data on the pedestal.

The result of our calculation for the APD in  $\Delta\eta$  is shown in Fig. 11 [20]. The two free parameters  $\sigma_0$  and  $\Delta T$  are adjusted to get the good fit of the STAR data [19]; they are

$$\sigma_0 = 0.22, \quad \Delta T = 15 \text{ MeV/c} \quad . \quad (23)$$

The change from  $T_0$  to  $T$  is only 5%, so the difference is insignificant in the calculation of single-particle distribution. However, the difference is sufficient to give rise to a pedestal in  $\Delta\eta$ , whose origin is therefore the feedback from the lost energy of the hard parton to the hadrons through the enhanced thermal medium. It should be recognized that the good fit in Fig. 11 is not a trivial consequence of the use of two parameters, since the height of the peak is the result of multidimensional integrals involving many components of recombination.

With the parameters in (23) fixed the APD in  $\Delta\phi$  can be calculated; the result is shown in Fig. 12 [20]. The dashed line corresponds to the pedestal in  $\Delta\eta$ , but is forced to vanish at  $|\Delta\phi| = 1$  because of the subtraction scheme. The solid line includes the  $\mathcal{TS}$  contribution on top of the pedestal and exhibits good agreement with the data [19]. The yield of the AP has been studied in [21] on the basis of some correlation among the soft partons.

Although we have not put in by hand any short- or long-range correlation, one may interpret the correlation of the shower partons exhibited in Fig. 5 as an intrinsic short-range correlation in a jet, and the feedback mechanism of the energy loss of hard partons to the enhancement of thermal partons as a form of long-range correlation. Through parton recombination these correlations are transmitted from the partons to the hadrons that are measured.

The advantage of studying the particles associated with triggers is that the details of the jet structure become manifest and allow us to determine the properties of the shower partons, such as  $\sigma_0$  in (23). The drawback is the necessity of making subtraction of the background that may involve some ambiguity. A way to avoid the drawback is to study autocorrelation in  $\Delta\eta$  and  $\Delta\phi$  starting with either (11) or (17), in which the two particles are treated on equal footing and no subtraction beyond the definition of  $C_2(1, 2)$  is needed. That will be our next project, in which we can use the results of [20] as the basis for the calculation of the autocorrelation in  $\Delta\eta$  and  $\Delta\phi$  within a definite  $p_T$  range.

## 5. Concluding remarks

In conclusion, it is worth stressing that parton recombination provides a framework to describe correlation at intermediate  $p_T$  range. So far we have not assumed any exotic correlation among the partons, since none seems necessary. However, some dynamical correlation may be present when probed properly, in which case our formalism may be well suited to decipher its characteristics. Of course, it is the correct hadronization process that must first be established. After that we can then investigate not only the detail properties of the correlation in the near-side jet, but also the nature of jet quenching on the away side.

I am grateful to Gunther Roland and Tom Trainor for inviting me to this very stimulating workshop on Correlations and Fluctuations. I also want to thank my collaborators, C. B. Chiu, R. Fries, Z. Tan and C. B. Yang, who have been crucial in the completion of the work reviewed here, so the credit for the success of our approach should go mostly to them, without whom there are no results to show. This work was supported in part, by the U. S. Department of Energy under Grant No. DE-FG02-96ER40972.

- [1] Hwa R C and Yang C B 2004 *Phys. Rev. C* **71** 024905
- [2] Hwa R C and Yang C B 2004 *Phys. Rev. C* **70** 024904
- [3] Hwa R C and Yang C B 2002 *Phys. Rev. C* **66** 025205
- [4] Srivastava D, Gale C and Fries R 2003 *Phys. Rev. C* **67** 034903
- [5] Hwa R C and Tan Z nucl-th/0503052.
- [6] Adler S (PHENIX Collaboration) 2003 *Phys. Rev. Lett.* **91** 072301
- [7] Adler S (PHENIX Collaboration) 2004 *Phys. Rev. C* **69** 034909
- [8] Hwa R C and Yang C B 2004 *Phys. Rev. C* **67** 034902
- [9] Greco V, Ko C and Lévai P 2003 *Phys. Rev. Lett.* **90** 202302; 2003 *Phys. Rev. C* **68**, 034904
- [10] Fries R, Müller B, Nonaka C and Bass S 2003 *Phys. Rev. Lett.* **90** 202303 ; 2003 *Phys. Rev. C* **68** 044902
- [11] Cronin J et al 1975 *Phys. Rev. D* **11** 3105; Antreasyan D et al 1979 *Phys. Rev. D* **19** 764
- [12] Hwa R C and Yang C B 2004 *Phys. Rev. Lett.* **93** 082302; *Phys. Rev. C* **70**, 037901.
- [13] Matathias F (for PHENIX Collaboration) 2004 *J. Phys. G: Nucl. Part. Phys.* **30** S1113
- [14] Arsene I et al (BRAHMS Collaboration) 2004 *Phys. Rev. Lett.* **93** 242303
- [15] Hwa R C and Yang C B and Fries R J 2005 *Phys. Rev. C* **71** 024902
- [16] See contributions by Ray L and Trainor T in these proceedings
- [17] Hwa R C and Tan Z nucl-th/0503060
- [18] Hwa R C and Yang C B 2004 *Phys. Rev. C* **70** 054902
- [19] Wang F (for STAR collaboration) nucl-th/0501016 see contribution in these proceedings
- [20] Chiu C B and Hwa R C nucl-th/0505014
- [21] Fries R, Bass S and Müller S 2005 *Phys. Rev. Lett.* **94** 122301